environmental microbiology reports

Environmental Microbiology Reports (2018) **10**(6), 663–672 doi:10.1111/1758-2229.12678

Electron donor-driven bacterial and archaeal community patterns along forest ring edges in Ontario, Canada

Konstantin von Gunten,[1*] Stewart M. Hamilton,[2] Cheng Zhong,[1] Camilla Nesbø,[3] Jiaying Li,[3] Karlis Muehlenbachs,[1] Kurt O. Konhauser[1] and Daniel S. Alessi[1]

[1]*University of Alberta, Earth and Atmospheric Sciences, 1-26 Earth Sciences Building, Edmonton, Alberta, T6G 2E3, Canada.*

[2]*Ministry of Northern Development and Mines, Sudbury Office, 159 Cedar Street, Sudbury, Ontario, P3E 6A5, Canada.*

[3]*University of Alberta, Biological Sciences, 11455 Saskatchewan Drive, Edmonton, Alberta, T6G 2E9, Canada.*

Summary

Forest rings are 50–1600 m diameter circular structures found in boreal forests around the globe. They are believed to be chemically reducing chimney features, having an accumulation of reduced species in the middle of the ring and oxidation processes occurring at the ring's edges. It has been suggested that microorganisms could be responsible for charge transfer from the inside to the outside of the ring. To explore this, we focused on the changes in bacterial and archaeal communities in the ring edges of two forest rings, the 'Bean' and the 'Thorn North' ring, in proximity to each other in Ontario, Canada. The drier samples from the methane-sourced Bean ring were characterized by the abundance of bacteria from the classes Deltaproteobacteria and Gemmatimonadetes. *Geobacter* spp. and methanotrophs, such as *Candidatus Methylomirabilis* and *Methylobacter*, were highly abundant in these samples. The Thorn North ring, centred on an H_2S accumulation in groundwater, had wetter samples and its communities were dominated by the classes Alphaproteobacteria and Anaerolineae. This ring's microbial communities showed an overall higher microbial diversity supported by higher available free energy. For both rings, the species diversity was highest near the borders of the 20–30 m broad ring edges.

Received 26 March, 2018; accepted 8 July, 2018. *For correspondence. E-mail vongunte@ualberta.ca; Tel. +1 780 492 3265; Fax +1 780 492 2030.

Introduction

Circular features, also known in Canada as 'forest rings', are clearly visible in air photos and satellite images due to lower tree densities and the formation of a depression (up to 3 m deep) on the ring edge, which can be 10–30 m in thickness (Brauneder *et al*., 2016). A number of theories have been proposed for forest ring formation, including the drainage of thermokarst lakes (thaw basins), the collapse of peat plateaus after the melting of covering ice (Mollard, 1980), or the presence of kimberlites or other mineral deposits within the ring (Brauneder *et al*., 2016). It was shown that the rings are similar to 'reduced chimneys' in terms of shape and geochemistry that form over mineral deposits and oil and gas accumulations (Pirson, 1981; Hamilton *et al*. 2004a, b; Cameron *et al*. 2004; Kelley *et al*. 2006; Klusman, 2009). All rings studied to date are centred on accumulations of chemical reductants (e.g., methane, hydrogen sulfide) in soil and rock (Hamilton *et al*., 2004c). Oxidation processes linked to these reduced species on the surface are responsible for the generation of acidity and the formation of a swampy depression (ring edge) due to carbonate dissolution (Veillette and Giroux, 1999; Hamilton and Hattori, 2008). It has also been suggested that microorganisms might contribute to the ring formation by promoting oxidation of the reduced chemical species (Hamilton and Govett, 2010). However, to our knowledge soil microbial profile in forest rings has never been investigated.

In this study, we investigate two forest rings located in Northern Ontario, Canada (Supplementary Information Fig. S1). The first is the 430 m wide 'Bean' ring, 60 km northwest of Hearst, which is located over carbonate-rich till with numerous sand lenses and a peat layer (up to 5 m) on top. The primary reductant in this ring is methane, similar to eight other rings located nearby (Hamilton *et al*., 2004c). For details see Supplementary Information. The second is the 560 m wide 'Thorn North' ring located 45 km northwest of Timmins, which overlies an upward

sequence of glaciolacustrine clay and clayey till, glaciolacustrine sands (~0.3 m), and peat (Brauneder *et al*., 2016). Hydrogen sulfide was found to be the primary reductant in this ring. The purpose of this study is to investigate the role of microorganisms in these two forest rings using 16S rRNA gene sequencing, geochemical and isotopic investigations, and statistical analyses.

Results

Site characteristics and geochemical parameters

At both rings the major surface cover was peat, with highly variable thicknesses ranging from 30 to 180 cm (Table 1). The average peat thickness was greater along the Thorn North edges with 103 ±18 cm and 178 ± 2 cm for transect 1 and 2 (see maps in Supplementary Information Fig. S1) respectively. The average peat thickness in the Bean ring was 59 ± 20 cm and 82 ± 15 cm for the two transects. At the points of sampling, the Thorn North samples had a higher average moisture content of 30% ± 12% versus 21% ± 3% at the Bean ring. The pH was similar in both rings: 6.7 ± 0.6 in the Bean ring, and 6.5 ± 0.6 in the Thorn North ring, and expressed an inverse relationship to the moisture content. Major plant species were recorded and are described in the Supplementary Information.

The metal distribution along ring edges, determined by aqua regia digestion, varied greatly (Table 1; more details in Supplementary Information Tables S1 and S2). Ca and Mg concentrations were generally higher on the borders of the ring edge and lower in the middle (Supplementary Information Fig. S2), consistent with previously described carbonate dissolution (Brauneder *et al*., 2016). Sulfur (Supplementary Information Fig. S2) was abundant in the Thorn North soils (up to 885 ppm) and was in general low on the ring edge borders (as low as 81 ppm). $CaCl_2$ extraction released few metals from the Bean ring samples, suggesting low mobility of those metals (Supplementary Information Table S1). Transition metals, such as Co, Ni and Cu, were more abundant in the exchangeable fraction of the Thorn North soils, averaging 0.27 ± 0.14, 0.30 ± 0.07 and 0.17 ± 0.07 ppm respectively (Supplementary Information Table S2). In the Bean ring the concentrations of those metals were considerably lower, that is, 0.07 ± 0.03, 0.06 ± 0.01 and 0.07 ± 0.03 ppm respectively.

Gas concentrations and isotopic signatures

In the Bean ring, gas measurements indicated an oxygen drop (from 20.9% to 20.2%) and a carbon dioxide spike (from 0.2% to 1.0%) on the inner edge of transect 1 (Supplementary Information Fig. S2). In transect 2 of the Thorn North ring, a similar but less pronounced oxygen drop (20.9%–20.7%) with a carbon dioxide spike (0.2%–0.5%) was observed, suggesting that respiration in the first layers of the mineral soil is strongest on the inner edge of the rings. $\delta^{13}C\text{-}CO_2$ was typical for soils, ranging from −8.8‰ to −22.4‰. Most samples did not have sufficiently high CH_4 concentrations to conduct isotopic measurements. However, in the Bean ring, $\delta^{13}C\text{-}CH_4$ was measured for the outer edge of transect 1 and the inner edge of transect 2, having values of −56‰ and −79‰ respectively (Table 1). The inner edge reading was similar to that reported by Hamilton *et al*. (2004c) for the methane at the centre of the ring (−81.2 ± 4.9‰) but $\delta^{13}C\text{-}CH_4$ for the outer edge was isotopically heavier. In the Thorn North ring, trace amounts of methane were measured in samples from the inner edge and in the middle of the ring edge of transect 2, with a $\delta^{13}C$ of −120‰ and −116‰ respectively. The sulfate in water from shallow (8 m) monitoring wells at Thorn North centre had a $\delta^{34}S\text{-}SO_4^{2-}$ of −13.2‰ ± 1.1‰ (n = 4) Canyon Diablo Troilite (CDT). For $\delta^{34}S\text{-}S^{2-}$, a value of −18.5‰ ± 3.5‰ (n = 2) CDT was determined.

Microbial community and diversity

In Bean ring, Deltaproteobacteria, Nitrospira, Gemmatimonadetes and Betaproteobacteria were the dominant classes, while in Thorn North, the community was dominated by Alphaproteobacteria, Anaerolineae, Betaproteobacteria and Nitrospira (Fig. 1). A comparison of these microbial communities to other peatlands can be found in the Supplementary Information.

In the Bean ring samples, OTU1 classified as *Geobacter* was the most abundant in the Bean ring samples, comprising 0.03%–27.44% of all reads (Table 2). Also highly abundant, especially in the Bean ring transect 2 (2.19%–7.26%), was a sequence related to *0319-6A21*, an uncultured bacterium of the class Nitrospirales, which is thought to be involved in nitrification (Lavoie *et al*., 2017). The third most abundant OTU may also be linked to the nitrogen cycle, as it was related to the Deltaproteobacterial taxon *43F-1404R*, which has been suggested to carry out denitrification (Rasigraf *et al*., 2017). Another abundant OTU, OTU16, was related to *Ferriphaselus*, an Fe(II)-oxidizing Betaproteobacteria (Chan *et al*., 2016). At the Thorn North site, the most abundant OTU (0.33%–5.48%, mostly in transect 2) was assigned to the phylum Atribacteria, which are mainly bacteria performing primary or secondary fermentation under strictly anaerobic conditions (Nobu *et al*., 2016). Several OTUs important in Thorn North samples belonged to the Miscellaneous Creanarchaeotic Group (0.00%–6.21%). The major metabolism associated with this group is likely chemoheterotrophy (Fillol *et al*., 2015) and not linked to methane oxidation (Kubo *et al*., 2012). OTU12 (0.00%–3.18%, mostly transect 2) was classified as *Ralstonia*, an Fe(II)-oxidizing Betaproteobacteria. The full list of assigned OTUs can be found in the Appendix S1.

Table 1. Summary of major geochemical parameters for the collected samples.

Sample	Transect	Dist (m)	Depth (cm)	pH	Water (%)	S (μg g^{-1})	Ca (mg g^{-1})	Fe (mg g^{-1})	Co (μg g^{-1})	Ni (μg g^{-1})	Cu (μg g^{-1})	Zn (μg g^{-1})	$\delta^{13}CO_2$ (‰)	$\delta^{13}CH_4$ (‰)	Diversity
BE1IN1	B (NW)	−7	95–105	7.28	18	91.1	29.1	12.6	6.3	17.5	22.5	96.4	−19.1	–	138.06
BE1ED1	B (NW)	0	76–96	7.43	14	74.1	32.4	9.5	5.0	14.1	11.2	55.9	−20.0	–	149.10
BE1ED2	B (NW)	5	40–60	6.35	27	76.3	2.3	25.8	10.7	33.4	14.2	283.2	–	–	72.81
BE1ED3	B (NW)	10	40–60	7.34	19	63.9	1.9	16.3	7.8	21.4	9.7	45.3	−17.7	–	50.08
BE1ED4	B (NW)	15	40–60	5.93	21	65.5	2.4	23.8	14.8	30.5	17.4	143.6	–	–	29.96
BE1ED5	B (NW)	20	50–70	6.79	18	51.8	2.0	14.5	7.7	20.5	12.5	70.8	−18.9	–	12.22
BE1OUT1	B (NW)	27	30–50	5.92	21	76.2	2.8	27.3	13.8	37.3	24.8	95.5	−22.4	−56.4	20.63
BE2IN1	B (NE)	−11	90–105	7.28	23	99.4	9.5	16.5	8.1	21.2	14.0	83.2	−16.7	−79.2	86.80
BE2ED1	B (NE)	0	60–80	6.16	21	134.3	2.5	20.0	10.8	25.8	13.7	175.1	–	–	26.05
BE2ED2	B (NE)	4	100–105	7.36	18	74.9	17.7	18.1	9.2	23.5	17.8	291.4	−10.0	–	60.71
BE2ED3	B (NE)	8	95–110	7.18	18	63.9	4.7	19.6	11.1	25.5	13.4	141.0	–	–	n.s.
BE2ED4	B (NE)	12	75–85	6.47	26	205.1	3.3	22.5	11.9	31.6	22.5	84.3	–	–	46.61
BE2ED5	B (NE)	17	58–78	5.78	26	242.9	3.7	29.3	14.7	31.2	15.4	139.0	−18.4	–	44.95
BE2ED6	B (NE)	21	85–105	6.62	19	54.1	11.8	19.7	11.3	29.0	24.0	129.0	–	–	132.78
BE2OUT1	B (NE)	32	92–102	6.99	20	124.4	2.4	15.9	9.7	24.4	19.9	57.1	−13.9	–	93.20
TN1IN1	TN (N)	−10	100–120	5.56	32	331.2	2.1	4.8	2.8	8.0	6.8	71.6	−8.8	–	184.77
TN1ED1	TN (N)	0	100–120	5.78	47	378.0	2.3	3.0	1.1	4.1	4.2	82.5	−12.1	–	169.92
TN1ED2	TN (N)	11	100–120	5.5	58	481.5	3.6	3.9	1.7	5.6	5.3	31.7	–	–	147.71
TN1ED3	TN (N)	20	80–100	6.3	27	81.1	2.2	4.9	3.4	6.9	4.8	19.4	–	–	162.21
TN1OUT1	TN (N)	30	135–145	7.18	19	110.7	3.3	5.5	3.2	8.3	11.3	36.7	−16.9	–	295.95
TN2IN1	TN (W)	−10	180–190	7.21	20	295.7	3.7	3.1	2.1	6.2	3.8	25.5	−17.4	−120.2	99.12
TN2ED1	TN (W)	0	175–180	6.44	21	197.8	4.6	3.9	2.4	6.9	3.8	73.4	−19.8	–	82.32
TN2ED2	TN (W)	10	180–185	6.93	28	471.1	1.8	4.9	2.9	8.7	4.1	121.2	−17.9	−115.9	99.37
TN2ED3	TN (W)	20	180–185	6.93	22	246.9	4.7	3.9	2.4	7.3	3.2	63.9	–	–	95.45
TN2OUT1	TN (W)	30	175–180	6.5	31	885.1	2.7	5.8	3.5	9.7	8.2	154.5	−11.0	–	116.14

Note the different concentration units for metals. The distance ('Dist') represents the relative distance to the inner edge after scaling the edge to a nominal thickness of 20 m as used in Fig. 1. The sampling depth represents the depth of the peat/mineral soil interface. For the diversity, the Inverse Simpson index is shown. More species richness and diversity parameters and detailed aqua regia and CaCl2 extraction results can be found in Tables S1–S3 (Supplementary Information). 'B': Bean ring. 'TN': Thorn North ring. 'n.s.': not sequenced.

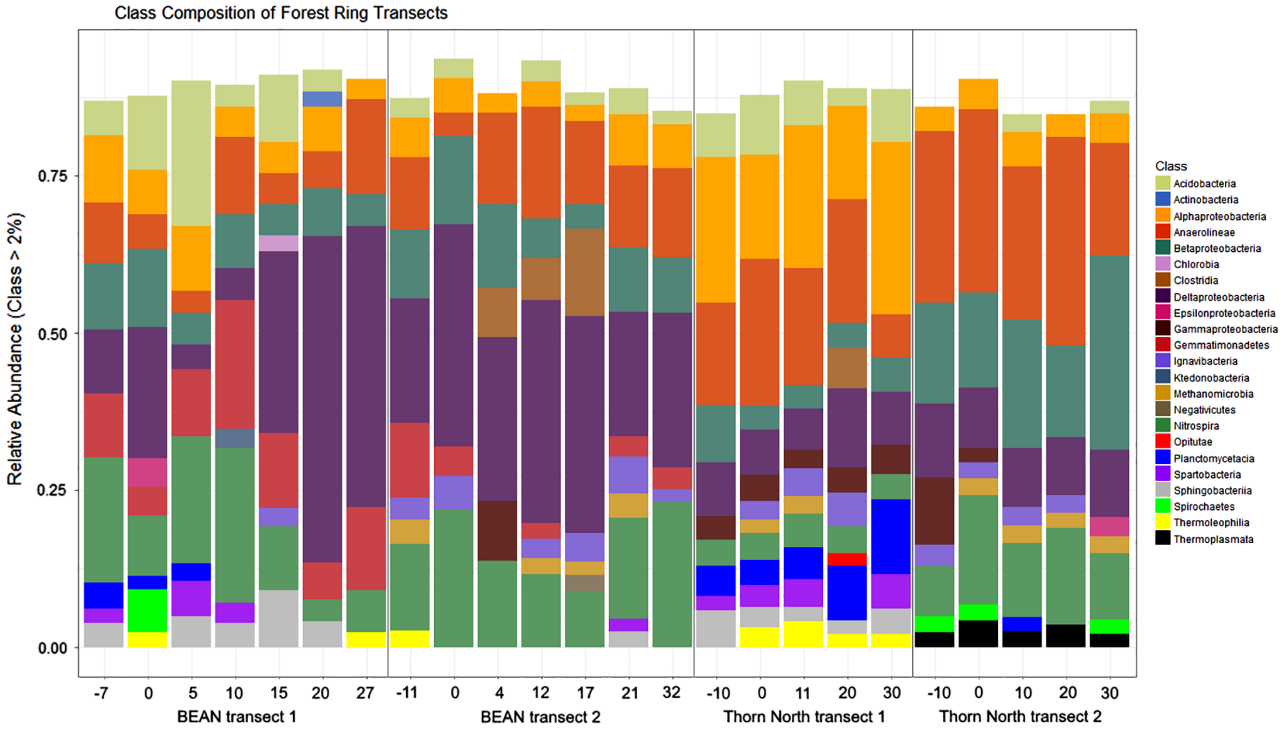

Fig. 1. 16S rRNA-based class composition summary of the ring transects after removal of unknowns, eukaryotic sequences and singletons. For each of the four transects, samples are ordered from the inside of the edge to the outside. The relative distance is given on the x-axis (scaled to a 20 m nominal edge width as shown in Table 1). Only classes with a relative abundance of > 2% are shown. In total, 855–2954 OTUs per sample were found (Supplementary Information Table S3). The distribution of the sample sequencing depth and the rarefaction curves are shown in Supplementary Information Figs. S3 and S4. See Supplementary Information Fig. S5 for phylum composition.

The Thorn North samples had a higher diversity than the Bean samples (Table 1 and Supplementary Information Table S3); Inverse Simpson indices for transect 1 and 2 of the Bean ring were 67.2 ± 51.6 and 70.2 ± 33.7, respectively, while the Thorn North had Inverse Simpson indices of 192.1 ± 53.3 and 98.5 ± 10.8 for transect 1 and 2 respectively. With the exception of Bean transect 1, higher diversity was generally found for samples at a close proximity to the inner and outer edges of each ring, with lower diversity within the ring edge itself. The differences in the community composition between transects were visualized using a constrained ordinations plot (Fig. 2).

Predicted metabolisms

In all transects, predicted metabolism analysis (Supplementary Information Fig. S7) indicated a high abundance of OTUs related to sulfate reducers, comprising on average 11% of all sequences, with slightly increased values at the boundaries of the ring edge. Furthermore, OTUs associated with nitrite reducers and ammonia oxidizers, with average abundances of 11% and 14%, respectively, were found in all samples. In the Bean ring transects, sulfide oxidizers were remarkably well-represented at 6%–12%, followed by methanotrophs comprising 1%–12%. Examples of such predicted methanotrophs were relatives of the aerobic *Methylobacter*, *Methylocystic* and *Methylobacterium* genera (Belova *et al.,* 2013; Anesti *et al.,* 2004; Wartiainen *et al.,* 2006), the nitrate-reducing *Candidatus Methylomirabilis* (Wu *et al.,* 2012), and the archeon *Candidatus Methanoperedens* which is able to oxidize methane with nitrate, Fe(III) and Mn(IV) (Cui *et al.,* 2015). The abundance of OTUs consistent with methanotrophy was variable across the Bean ring transects, with the highest abundance generally being in the middle of the ring edges. OTUs related to methanotrophs were not highly abundant in the Thorn North ring transects (0%–4%). However, the Thorn North ring had a similar abundance of sulfide oxidizers (5%–10%) compared with the Bean ring.

Discussion

The higher microbial diversity found in samples form Thorn North ring may be related to the availability of hydrogen sulfide as an electron donor. The energy gain from direct oxidation of HS^- with oxygen under normal surface conditions is higher as compared with the oxidation of methane (Robie *et al*., 1978). In addition, sulfur oxidation could be coupled to denitrification and ammonia oxidation, allowing for a more direct use of the energy

Table 2. Summary of the top OTUs for the Bean ring samples (top) and the Thorn North ring samples (bottom), ordered based on their total amount of counts.

	Bean (%)		Thorn North (%)		
	Tran 1	Tran 2	Tran 1	Tran 2	Taxonomy
Top 10 Bean OTUs					
Otu1	7.6%	6.9%	0.0%	0.0%	Bacteria; Proteobacteria; Deltaproteobacteria; Desulfuromonadales; Geobacteraceae; *Geobacter*
Otu5	1.7%	3.3%	0.4%	0.1%	Bacteria; Nitrospirae; Nitrospira; Nitrospirales; 0319-6A21
Otu2	1.9%	2.7%	0.5%	0.2%	Bacteria; Proteobacteria; Deltaproteobacteria; 43F-1404R
Otu4	4.2%	0.3%	0.0%	0.0%	Bacteria; Proteobacteria; Deltaproteobacteria; GR-WP33-30
Otu8	2.2%	2.2%	0.7%	0.1%	Bacteria; Acidobacteria; Holophagae; Subgroup-7
Otu16	0.7%	2.2%	0.3%	0.7%	Bacteria; Proteobacteria; Betaproteobacteria; Nitrosomonadales; Gallionellaceae; *Ferriphaselus*
Otu6	0.1%	2.7%	0.1%	0.1%	Bacteria; Proteobacteria; Deltaproteobacteria; Desulfuromonadales; BVA18
Otu11	0.8%	2.0%	0.0%	0.0%	Bacteria; Acidobacteria; Holophagae; Subgroup-7
Otu149	1.1%	1.5%	1.0%	0.1%	Bacteria; Chloroflexi; KD4-96
Otu36	1.6%	0.7%	1.1%	0.1%	Bacteria; Acidobacteria; Acidobacteria; Subgroup-6
Top 10 Thorn North OTUs					
Otu3	0.0%	0.0%	1.2%	4.4%	Bacteria; Atribacteria
Otu17	0.2%	1.2%	2.0%	2.9%	Archaea; Miscellaneous-Crenarchaeotic-Group
Otu9	0.0%	0.9%	2.8%	1.8%	Bacteria; Proteobacteria; Deltaproteobacteria; Sva0485
Otu10	0.0%	0.0%	0.0%	3.1%	Archaea; Miscellaneous-Crenarchaeotic-Group
Otu33	0.0%	0.0%	0.1%	2.5%	Archaea; Miscellaneous-Crenarchaeotic-Group
Otu22	0.0%	0.2%	0.6%	1.6%	Bacteria; Actinobacteria; OPB41
Otu12	0.3%	0.3%	0.0%	2.1%	Bacteria; Proteobacteria; Betaproteobacteria; Burkholderiales; Burkholderiaceae; *Ralstonia*
Otu19	0.2%	2.1%	1.4%	0.6%	Bacteria; Bacteroidetes; Bacteroidetes-vadinHA17
Otu66	0.0%	0.1%	0.5%	1.5%	Bacteria; Proteobacteria; Deltaproteobacteria; Sva0485
Otu49	0.0%	0.0%	0.3%	1.5%	Bacteria; Planctomycetes; Phycisphaerae; MSBL9

The percentages represent the average relative abundance of the respective sequence in each transect. 'Tran': transect. For a complete OTU list, see Appendix S1.

(Syed *et al*., 2006). This overall higher energy availability allows the Thorn North microbial environment to reach greater species richness and diversity compared with the Bean ring (Evans *et al*., 2005). Highest species diversity was generally found on the borders of the ring edge, which were previously shown to be locations of the highest redox gradients across the entire rings (Brauneder *et al*., 2016). Higher redox gradients generally favour higher energy throughput and would support higher species abundance (Lipson *et al*., 2015).

The constrained ordinations plot (Fig. 2) suggests that soil moisture, and S content are correlated with the communities at Thorn North. The importance of the soil moisture in controlling microbial communities was previously described by Brockett *et al*. (2012) on a regional scale and demonstrated by Zhao *et al*. (2016) in field trials. Both studies demonstrated that soil moisture is likely the key factor determining the microbial composition. The correlation between exchangeable metals and soil moisture may be caused by greater leaching of metals in the wetter soil conditions found in the Thorn North ring (Zhao *et al*., 2016). Higher water content might also lead to less aerated soil conditions in Thorn North, which is supported by the taxonomic composition. For example, the class Gemmatimonadetes, abundant in the Bean ring samples, is preferably associated with drier soils (DeBruyn *et al*., 2011), while the wetter conditions in the Thorn North ring edge soil samples (Table 1) would be less suitable to those bacteria. The class Anaerolineae (phylum Chloroflexi) was shown to contain strictly anaerobic species (Yamada *et al*., 2006), and its relative abundance is higher in the wetter Thorn North samples.

Methane in the Bean ring likely originates from deeper layers (9–40 m) (Hamilton *et al*., 2004c; Brauneder *et al*., 2016). In agreement with this, we did not observe high relative abundance of methanogens (average 0.1%, Supplementary Information Fig. S7) in the Bean ring samples, although the major cofactors necessary for their metabolisms (Fe, Ni and Co; Glass and Orphan, 2012) were present. The predicted methanotrophs in the Bean ring (on average 5.2%), which were especially prominent closer to the inner side of the ring edge, may consume the methane originating from these deeper layers. Furthermore, the $\delta^{13}C$ for methane (Table 1) is consistent with active methanotrophy, resulting in the slightly heavier values (−79‰ to −59‰) observed in residual methane on the outer ring edge. The lack of deep methane in Thorn North likely led to an overall lower abundance of predicted methanotrophs (on average 1.5%), which in turn, facilitated lighter isotopic signatures of the detected methane (−120‰ to −116‰), which was likely produced by methanogens near the surface. As for the

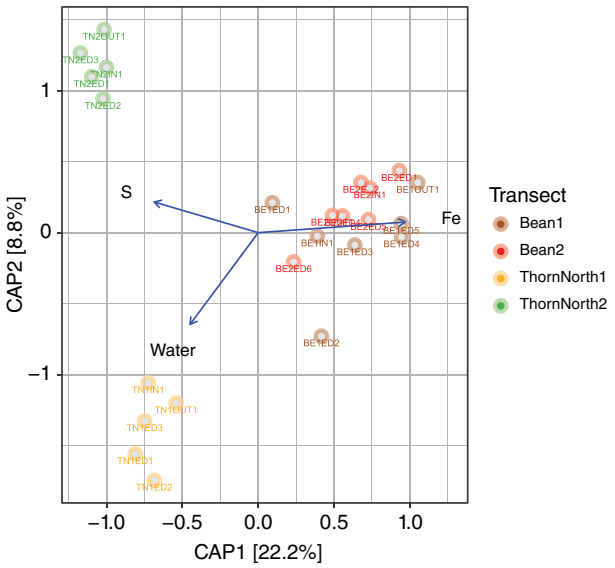

Fig. 2. Constrained ordinations plot. The tested environmental parameters are shown in Table 1. Only soil moisture ('Water'), S and Fe contents were significant, as determined by Permutational Multivariate Analysis of Variance (PERMANOVA, $p < 0.05$, see Supplementary Information Table S4 for details). The four colours represent the four transects and the arrows are indicating environmental factors. The clustering of the datasets in this plot is comparable to the principal coordinate analysis plot shown in Supplementary Information Fig. S6, suggesting that suggesting that the amount of chosen environmental variables for the statistical analysis was appropriate (Ramette, 2007).

δ^{13}C-CO_2, the average value was −16‰, a value lower than that of atmospheric CO_2 (−7 to −8‰) and within the range of CO_2 produced during the decay of plant matter (Fernandez *et al*., 2003; Konhauser, 2007). Fermentation processes, yielding typical δ^{13}C-CO_2 values around −9‰, likely caused the heavier isotopic signatures observed in some samples, which usually had higher water contents (Table 1).

Sulfur isotope measurements in the Thorn North ring indicated that the H_2S present cannot result directly from reduction of dissolved SO_4^{2-} at the site, because the δ^{34}S-S^{2-} is only slightly isotopically lighter than the δ^{34}S-SO_4^{2-}. The expected fractionation due to bacterial reduction of aqueous sulfate is at least −25‰ (Habicht and Canfield, 1997), which would lead to a starting isotopic composition for SO_4^{2-} of approximately +6.5‰, which is much higher than observed. However, the anticipated starting range matches well with the range for δ^{34}S-SO_4^{2-} in shield terrain (+6.0‰ ± 5.9‰, n = 159, unpublished data), found in a large regional groundwater study near Sudbury (Dell *et al*., 2016) and in local studies near mineral deposits in northeastern Ontario (+10.3‰ ± 4.3‰, n = 16; Fritz *et al*., 1994). A likely scenario is that the observed deep H_2S originally resulted from the bacterial reduction of aqueous SO_4^{2-} (δ^{34}S-SO_4^{2-} of approximately +6.5‰) in the ambient groundwater of the regional aquifers, yielding the observed (average) δ^{34}S-S^{2-} value of −18.5‰ for aqueous H_2S. The methane commonly observed in groundwater in the fine-grained glacial sediments of the Cochrane Till (Hamilton *et al*., 2004a,b,c) is evidence that reducing agents, likely in the form of buried organic material, are present in these glacial sediments. Where a local source of reducing agents and a regional aqueous sulfate source are both available, the biogenic production of aqueous sulfide would be biologically favoured over methanogenesis (Lovley *et al*., 1982), and this is consistent with the isotopic composition of the deep sulfide. The dissolved sulfide then migrates upward and outward from the ring centre and is subject to bacterial oxidation at the ring edge, which likely produces a minor fractionation of −2‰ to −6‰ (i.e., of a considerably lower magnitude than during sulfate reduction, Brabec *et al.,* 2012). The δ^{34}S-SO_4^{2-} is slightly isotopically heavier than δ^{34}S-S^{2-} by an average of 5.3‰. This may result from mixing of a lighter δ^{34}S-SO_4^{2-} product of sulfide oxidation with the isotopically heavier ambient sulfate in the shallow aquifer, to yield a final δ^{34}S-SO_4^{2-} that is slightly more positive than the δ^{34}S-S^{2-}.

As mentioned above, a *Geobacter* OTU was among the most abundant, particularly in the Bean ring (Table 2). *Geobacter* species are able to reduce Fe(III), as well as Mn(IV) and S^0, using electron conducting pili (Childers *et al*., 2002; Mahadevan *et al*., 2006; Prakash *et al*., 2010), and to live in syntrophic relationships with methanogens (Rotaru *et al*., 2014) might play an essential role in the forest ring soils communities. Particularly considering that Fe was suggested as a major environmental parameter in Bean ring's microbial communities (Fig. 2). Other community members, such as *Ralstonia* and *Ferrifaselus*, both Fe(II) oxidizers, might benefit from *Geobacter*'s Fe(III)-reducing activity. *Geobacter's* potential role in ring formation is further discussed in the Supplementary Information.

Overall, the two forest rings in northern Ontario, exposed to the same climate and having a similar geology, but fed by either methane or hydrogen sulfide, showed very different microbial communities along their redox-active edges. The ring edges hosted communities rich in microorganisms that were able to oxidize the source material, which was supported by isotopic investigations. While the current study gives new insights into the microbiological communities and their biogeochemical importance at the ring edge, future studies are necessary to decipher their potential role in ring formation. In the next step, we will use wider transects that bracket more of the ring edge. Additionally, deeper sampling at the ring centre would allow for characterization of material near to the reduced sources and would likely provide insights into their origin and relationship to bacteria and archaea.

Experimental procedures

Soil sampling

Sampling was conducted in August 2016. For each ring, two transects of the ring edge were chosen, similar to sampling conducted for previous geochemical investigations of the same locations (Hamilton *et al*., 2004c; Hamilton and Hattori, 2008; Brauneder *et al*., 2016). The Bean ring was sampled in the northwestern (transect 1) and the northeastern sectors (transect 2) as shown in Fig. 1. Thorn North ring was sampled in the northern (transect 1) and western sectors (transect 2). The ring edge location is known to within $\pm$5 m from previous ground and airborne surveys. In this study, the edges were identified by measuring with a hip-chain from the surveyed position of existing monitoring wells (see Supplementary Information Fig. S8 for details). For consistency, we focused on the top-most mineral soil, as the overlying peat likely developed after the formation of the rings and because previous studies indicated the strongest geochemical and electrochemical responses in the mineral soil (Hamilton and Hattori, 2008). On each transect, samples were taken after establishing the peat thickness and depth of the mineral soil using a hand auger. A second hole was created to the top of the mineral soil layer, after which 20 cm of mineral soil were recovered using a narrower soil spoon cleaned with 95% ethanol. A sterile knife was used to cut the mineral soil in pieces, which were placed into sampling containers as described further below. Samples for DNA analysis were collected in the first 2 cm of the mineral soil (clay in Bean ring, sand in Thorn North ring) and placed into 15 ml centrifuge tubes. The following 10 cm of mineral soil were placed into 50 ml centrifuge tubes for geochemical analyses. All tubes were sealed with Teflon tape and frozen on dry ice for transportation. Samples were transferred to a -20°C freezer where they were kept until further analysis.

16S-rRNA sequencing

DNA was isolated using the FastDNA™ SPIN Kit for soil (MP Biomedicals). 16S rRNA was amplified by polymerase chain reaction with primers targeting the V4 region. Details on sample preparation and sequencing are given in the Supplementary Information. Sequencing was performed at The Applied Genomics Core (TAGC) laboratory at the University of Alberta using Illumina MiSeq platform for pair-end reads and the Illumina NexteraXT library preparation kit. Data processing was performed using the MetaAmp version 2.0 (Dong *et al*., 2017), a server-bound pipeline based on Mothur (Schloss *et al*., 2009) with UPARSE clustering of OUTs (Edgar, 2013) at the 97% similarity level. Reference alignment was done to the SILVA version 123 database (Quast *et al*., 2013; Yilmaz *et al*., 2014). After removing singletons and eukaryotic sequences, a total of 9126 OTUs were assigned. PCoA and the constrained ordinations (Canonical Analysis of Principal Coordinates) plots were prepared with R version 3.4.1 using the PHYLOSEQ package to visualize the importance of environmental factors (Anderson and Willis, 2003; Ramette, 2007; McMurdie and Holmes, 2013; R Core Team, 2017). The distribution of predicted metabolisms was analyzed with the METAGENassist tool by Arndt *et al*. (2012). Raw sequencing data was uploaded onto the National Centre for Biotechnology Information (NCBI) database and can be found under the BioSample SAMN07782722 (accession numbers SRX3297044 to SRX3297067). The library names correspond to the sample labels used in this manuscript (Table 1).

Geochemical analysis

Water content of soil samples was determined by loss of weight after oven drying a 10 g sample of soil at 105°C for (24 h). After weighing, the dried samples were then disaggregated using a mortar and pestle and sieved through a 2 mm stainless steel sieve. About 0.1 g of each soil sample were digested in aqua regia using 6 ml 37% HCl (ACS grade, Fisher Scientific) and 2 ml 70% HNO_3 (trace metal grade, Fisher Scientific) at 130°C. The liquid was evaporated and the remains soaked in 2% HNO_3 and 0.5% HCl. pH was determined on soil samples dried at 40°C in an oven and by using a 0.01 M $CaCl_2$ (ACS grade, Fisher Scientific) solution, a soil:solution mass to volume ratio of 1:5. After 6 h equilibration time, the suspensions were centrifuged at 3000 rcf and the supernatant was prepared for the analysis giving the soluble/exchangeable trace metals (Houba *et al*., 1990; Kashem *et al*., 2007). All solutions were analyzed by ICP-MS/MS (8800 ICP-MS Triple Quadrupole system, Agilent) after filtration through 0.2 μm nylon syringe filter membranes (Agilent).

Gas and isotopic analyses

Gas samples were collected in the field at the same locations as the soil samples using a steel soil gas tube and a hand pump. The tube was inserted to just above the soil water level to prevent the water from entering the rod. The gas was sampled from 30 to 50 cm depth, depending on the soil water depth, and pumped into plastic Tedlar bags. Field measurements for CH_4, CO_2 and O_2 on selected samples were taken directly from Tedlar bags using an Eagle multi-gas meter (RKI Instruments). Carbon isotope measurements on the collected gases were made using an Agilent 6890 gas chromatograph

configured to a Finnegan Mat 252 stable isotope ratio mass spectrometer on continuous flow mode. The carbon isotope data are reported in the delta notation with respect to VPDB calibrated against NGS 1, 2 and 3 as well as NBS 18 and 19. Samples for sulfur isotopes of aqueous sulfate ($\delta^{34}S\text{-}SO_4$) and sulfide ($\delta^{34}S\text{-}S^{2-}$) in groundwater were collected and analyzed in 2006 from the centre of the Thorn North ring. Water was collected in polyethylene bottles using an inertial hand-pump from shallow monitoring wells, screened between 7.5 and 8.5 m depth. Sulfide was precipitated in the field using AgCl; SO_4 was precipitated using $BaCl_2$ in the laboratory after removal of any Ag_2S precipitate. Both types of precipitates were combusted in an Elemental Analyzer (Carlo Erba NA1500) to release SO_2 for $\delta^{34}S$ determination using a Finnegan Delta XL Isotope Ratio Mass Spectrometer. Duplicates had standard deviations of 3.5‰ and 4.9‰ for $\delta^{34}S\text{-}SO_4$ and $\delta^{34}S\text{-}S^{2-}$ respectively.

Acknowledgements

The authors would like to thank Olga Levner (University of Alberta) for her support in the laboratory, Brian Lanoil (University of Alberta) for his scientific advice, Keiko Hattori (University of Ottawa) for the *ex gratia* sulfur isotope analyzes, Neal McClenaghan for his support in the field, Greg Goss (University of Alberta) for lending equipment, and the anonymous reviewer for highly appreciated comments. The Ontario Geological Survey supported this project by facilitating the access to the rings and data from previous studies and field visits. This work was financially supported by a Natural Sciences and Engineering Research Council of Canada (NSERC) Discovery grant to D.S.A. (RGPIN-04134).

Conflict of interest

The authors declare no conflicts of interest.

References

Anderson, M.J., and Willis, T.J. (2003) Canonical analysis of principal coordinates: a useful method of constrained ordination for ecology. *Ecology* **84**: 511–525.

Anesti, V., Vohra, J., Goonetilleka, S., McDonald, I.R., Sträubler, B., Stackebrandt, E., *et al*. (2004) Molecular detection and isolation of facultatively methylotrophic bacteria, including Methylobacterium podarium sp. nov., from the human foot microflora. *Environ Microbiol* **6**: 820–830.

Arndt, D., Xia, J., Liu, Y., Zhou, Y., Guo, A.C., Cruz, J.A., *et al*. (2012) METAGENassist: a comprehensive web server for comparative metagenomics. *Nucleic Acids Res* **40**: W88–W95.

Belova, S.E., Kulichevskaya, I.S., Bodelier, P.L., and Dedysh, S.N. (2013) Methylocystis bryophila sp. nov., a facultatively methanotrophic bacterium from acidic sphagnum peat, and emended description of the genus Methylocystis (ex Whittenbury et al. 1970) Bowman et al. 1993. *Int J Syst Evol Microbiol* **63**: 1096–1104.

Brabec, M.Y., Lyons, T.W., and Mandernack, K.W. (2012) Oxygen and sulfur isotope fractionation during sulfide oxidation by anoxygenic phototrophic bacteria. *Geochim Cosmochim Acta* **83**: 234–251.

Brauneder, K., Hamilton, S.M., and Hattori, K. (2016) Geochemical processes in the formation of 'forest rings': examples of reduced chimney formation in the absence of mineral deposits. *Geochim Explor Environ Anal* **17**: 85–99.

Brockett, B. F., Prescott, C. E., and Grayston, S. J. (2012) Soil moisture is the major factor influencing microbial community structure and enzyme activities across seven biogeoclimatic zones in western Canada. *Soil Biology and Biochemistry* **44**: 9–20.

Cameron, E.M., Hamilton, S.M., Leybourne, M.I., Hall, G.E. M., and McClenaghan, M.B. (2004) Finding deeply-buried deposits using geochemistry. *Geochem Explor Environ Anal* **4**: 7–32.

Chan, C.S., Emerson, D., and Luther, G.W. (2016) The role of microaerophilic Fe-oxidizing micro-organisms in producing banded iron formations. *Geobiology* **14**: 509–528.

Childers, S.E., Ciufo, S., and Lovley, D.R. (2002) Geobacter metallireducens accesses insoluble Fe (III) oxide by chemotaxis. *Nature* **416**: 767–769.

Cui, M., Ma, A., Qi, H., Zhuang, X., and Zhuang, G. (2015) Anaerobic oxidation of methane: an 'active' microbial process. *MicrobiologyOpen* **4**: 1–11.

DeBruyn, J.M., Nixon, L.T., Fawaz, M.N., Johnson, A.M., and Radosevich, M. (2011) Global biogeography and quantitative seasonal dynamics of Gemmatimonadetes in soil. *Applied and Environmental Microbiology* **77**: 6295–6300.

Dell, K.M., Fudge, S.P., and Hamilton, S.M. (2016) The ambient groundwater geochemistry program: Sudbury area. In summary of fieldwork and other activities. Ontario Geological Survey Open File Report 6323. 32-1 to 32-11.

Dong, X., Kleiner, M., Sharp, C.E., Thorson, E., Li, C., Liu, D., and Strous, M. (2017) Fast and simple analysis of MiSeq amplicon sequencing data with MetaAmp. *Front Microbiol* **8**: 1461.

Edgar, R.C. (2013) UPARSE: highly accurate OTU sequences from microbial amplicon reads. *Nat Methods* **10**: 996–998.

Evans, K.L., Greenwood, J.J., and Gaston, K.J. (2005) Dissecting the species–energy relationship. *Proc R Soc Lond B: Biol Sci* **272**: 2155–2163.

Fernandez, I., Mahieu, N., and Cadisch, G. (2003) Carbon isotopic fractionation during decomposition of plant materials of different quality. *Global Biogeochem Cycles* **17**(3): 1075.

Fillol, M., Sànchez-Melsió, A., Gich, F., Borrego, M., and C. (2015) Diversity of miscellaneous Crenarchaeotic group archaea in freshwater karstic lakes and their segregation between planktonic and sediment habitats. *FEMS Microbiol Ecol* **91**(4): fiv020.

Fritz, P., Frape, S.K., Drimmie, R.J., Appleyard, E.C., and Hattori, K. (1994) Sulfate in brines in the crystalline rocks of the Canadian shield. *Geochim Cosmochim Acta* **58**: 57–65.

Glass, J.B., and Orphan, V.J. (2012) Trace metal requirements for microbial enzymes involved in the production and consumption of methane and nitrous oxide. *Front Microbiol* **3**: 61.

Habicht, K.S., and Canfield, D.E. (1997) Sulfur isotope fractionation during bacterial sulfate reduction in organic-rich sediments. *Geochim Cosmochim Acta* **61**: 5351–5361.

Hamilton, S.M., and Govett, G.J.S. (2010) Vertical dispersion of elements in thick transported cover above the Thalanga Zn-Pb-cu deposit, Queensland, Australia: evidence of redox-induced electromigration. *Spl Publ Soc Econ Geol* **15**: 391–395.

Hamilton, S.M., and Hattori, K.H. (2008) Spontaneous potential and redox responses over a forest ring. *Geophysics* **73**: B67–B75.

Hamilton, S.M., Cameron, E.M., McClenaghan, E.M., and Hall, G.E.M. (2004a) Redox, pH and SP variation over mineralization in thick glacial overburden (I): methodologies and field investigation at marsh zone gold property. *Geochem Explor Environ Anal* **4**: 45–58.

Hamilton, S.M., Cameron, E.M.,, McClenaghan, E.M., and, Hall, G.E.M. (2004b) Redox, pH and SP variation over mineralization in thick glacial overburden (II): field investigations at the cross Lake VMS property. *Geochem Explor Environ Anal* **4**: 33–44,

Hamilton, S.M., Burt, A.K., Hattori, K.H., and Shirota, J. (2004c) The distribution and source of forest ring-related methane in northeastern Ontario. In summary of fieldwork and other activities (extended). Ontario Geological Survey Open File Report 6145. 21-1 to 21-26.

Houba, V.J.G., Novozamsky, I., Lexmond, T.M., and Van der Lee, J.J. (1990) Applicability of 0.01 M CaCl2 as a single extraction solution for the assessment of the nutrient status of soils and other diagnostic purposes. *Commun Soil Sci Plant Anal* **21**: 2281–2290.

Kashem, M.A., Singh, B.R., Kondo, T., Huq, S.I., and Kawai, S. (2007) Comparison of extractability of cd, cu, Pb and Zn with sequential extraction in contaminated and non-contaminated soils. *Int J Environ Sci Technol* **4**: 169–176.

Kelley, D.L., Kelley, K.D., Coker, W.B., Caughlin, B., and Doherty, M.E. (2006) Beyond the obvious limits of ore deposits: the use of mineralogical, geochemical, and biological features for the remote detection of mineralization. *Econ Geol* **101**: 729–752.

Klusman, R.W. (2009) Transport of ultratrace reduced gases and particulate, near-surface oxidation, metal deposition and adsorption. *Geochem Explor Environ Anal* **9**: 203–213.

Konhauser, K.O. (2007) *Introduction to Geomicrobiology*. New York, NY: John Wiley and Sons.

Kubo, K., Lloyd, K.G., Biddle, J.F., Amann, R., Teske, A., and Knittel, K. (2012) Archaea of the miscellaneous Crenarchaeotal group are abundant, diverse and widespread in marine sediments. *ISME J* **6**: 1949–1965.

Lavoie, K.H., Winter, A.S., Read, K.J., Hughes, E.M., Spilde, M.N., and Northup, D.E. (2017) Comparison of bacterial communities from lava cave microbial mats to overlying surface soils from lava beds National Monument, USA. *PloS One* **12**: e0169339.

Lipson, D.A., Raab, T.K., Parker, M., Kelley, S.T., Brislawn, C.J., and Jansson, J. (2015) Changes in microbial communities along redox gradients in polygonized Arctic wet tundra soils. *Environ Microbiol Rep* **7**: 649–657.

Lovley, D.R., Dwyer, D.F., and Klug, M.J. (1982) Kinetic analysis of competition between sulfate reducers and methanogens for hydrogen in sediments. *Appl Environ Microbiol* **43**: 1373–1379.

Mahadevan, R., Bond, D.R., Butler, J.E., Esteve-Núñez, A., Coppi, M.V., Palsson, B.O., *et al*. (2006) Characterization of metabolism in the Fe (III)-reducing organism Geobacter sulfurreducens by constraint-based modeling. *Appl Environ Microbiol* **72**: 1558–1568.

McMurdie, P.J., and Holmes, S. (2013) Phyloseq: an R package for reproducible interactive analysis and graphics of microbiome census data. *PLoS One* **8**: e61217.

Mollard, J.D. (1980) *Landforms and surface materials of canada: a stereoscopic atlas and glossary*, 6th ed. Saskatchewan, Canada: Regina.

Nobu, M.K., Dodsworth, J.A., Murugapiran, S.K., Rinke, C., Gies, E.A., Webster, G., *et al*. (2016) Phylogeny and physiology of candidate phylum 'Atribacteria'(OP9/JS1) inferred from cultivation-independent genomics. *ISME J* **10**: 273.

Pirson, S.J. (1981) Significant advances in magnetoelectrical exploration. In *Unconventional Methods in Exploration for Petroleum and Natural Gas*. Gottlieb, B. (ed). Dallas, TX: Southern Methodist University Press, pp. 169–196.

Prakash, O.M., Gihring, T.M., Dalton, D.D., Chin, K.J., Green, S.J., Akob, D.M., *et al*. (2010) Geobacter daltonii sp. nov., an Fe (III)-and uranium (VI)-reducing bacterium isolated from a shallow subsurface exposed to mixed heavy metal and hydrocarbon contamination. *Int J Syst Evol Microbiol* **60**: 546–553.

Quast, C., Pruesse, E., Yilmaz, P., Gerken, J., Schweer, T., Yarza, P., *et al*. (2013) The SILVA ribosomal RNA gene database project: improved data processing and web-based tools. *Nucleic Acids Res* **41**: D590–D596.

R Core Team. (2017) *R: A language and environment for statistical computing*. Vienna, Austria: R Foundation for Statistical Computing [WWW document]. URL https://www.R-project.org/.

Ramette, A. (2007) Multivariate analyses in microbial ecology. *FEMS Microbiol Ecol* **62**: 142–160.

Rasigraf, O., Schmitt, J., Jetten, M.S., and Lüke, C. (2017) Metagenomic potential for and diversity of n-cycle driving microorganisms in the bothnian sea sediment. *MicrobiologyOpen* **6**: 1–3.

Robie, R.A., Hemingway, B.S., and Fisher, J.R. (1978) Thermodynamic properties of minerals and related substances at 298. 15 K and 1 bar (10 ̄5 pascals) pressure and at higher temperatures. United States Geological Survey, USGS-BULL-1452.

Rotaru, A.E., Shrestha, P.M., Liu, F., Markovaite, B., Chen, S., Nevin, K.P., and Lovley, D.R. (2014) Direct interspecies electron transfer between Geobacter metallireducens and Methanosarcina barkeri. *Appl Environ Microbiol* **80**: 4599–4605.

Schloss, P.D., Westcott, S.L., Ryabin, T., Hall, J.R., Hartmann, M., Hollister, E.B., *et al*. (2009) Introducing mothur: open-source, platform-independent, community-supported software for describing and comparing microbial communities. *Appl Environ Microbiol* **75**: 7537–7541.

Syed, M., Soreanu, G., Falletta, P., and Béland, M. (2006) Removal of hydrogen sulfide from gas streams using biological processes - a review. *Can Biosyst Eng* **48**: 2.

Veillette, J.J., and Giroux, J.F. (1999) *The Enigmatic Rings of the James Bay Lowland: A Probable Geological Origin*. Canada: Natural Resources Canada, Geological Survey of Canada.

Wartiainen, I., Hestnes, A.G., McDonald, I.R., and Svenning, M.M. (2006) Methylobacter tundripaludum sp. nov., a methane-oxidizing bacterium from Arctic wetland soil on the Svalbard islands, Norway (78 N). *Int J Syst Evol Microbiol* **56**: 109–113.

Wu, M.L., van Teeseling, M.C., Willems, M.J., van Donselaar, E.G., Klingl, A., Rachel, R., *et al*. (2012) Ultrastructure of the denitrifying methanotroph 'Candidatus Methylomirabilis oxyfera,' a novel polygon-shaped bacterium. *J Bacteriol* **194**: 284–291.

Yamada, T., Sekiguchi, Y., Hanada, S., Imachi, H., Ohashi, A., Harada, H., and Kamagata, Y. (2006) Anaerolinea thermolimosa sp. nov., Levilinea saccharolytica gen. Nov., sp. nov. and Leptolinea tardivitalis gen. Nov., sp. nov., novel filamentous anaerobes, and description of the new classes Anaerolineae classis nov. and Caldilineae classis nov. in the bacterial phylum Chloroflexi. *Int J Syst Evol Microbiol* **56**: 1331–1340.

Yilmaz, P., Parfrey, L.W., Yarza, P., Gerken, J., Pruesse, E., Quast, C., *et al*. (2014) The SILVA and 'all-species living tree project (LTP)' taxonomic frameworks. *Nucleic Acid Res* **42**: D643–D648.

Zhao, C., Miao, Y., Yu, C., Zhu, L., Wang, F., Jiang, L., *et al*. (2016) Soil microbial community composition and respiration along an experimental precipitation gradient in a semiarid steppe. *Sci Rep* **6**: 24317.

Supporting Information

Additional Supporting Information may be found in the online version of this article at the publisher's web-site:

Appendix S1: Full taxonomic assembly
Appendix S2: Supplementary Information